

Korean red ginseng extracts alleviate skin damage in heat-stimulated skin cells by suppressing NF- κ B activation

Jeeyoung Kim¹, Weon Jeong Bang¹, Yung Hyup Joo¹, Sung Hyeon Lee¹ and Chang-Seok Lee^{2,3,*}

¹Research and Development Center, Durae Corporation, Anyang Trade Center 14F, 161, Simin-daero, Dongan-gu, Anyang, Gyeonggi-do, 14048, Republic of Korea

²Department of Senior Healthcare, Eulji University, Sujeong-gu, Seongnam, Gyeonggi-do 13135, Republic of Korea

³Cosmetic Science Major, Eulji University, Sujeong-gu, Seongnam, Gyeonggi-do 13135, Republic of Korea

*Corresponding author: kingderm21@naver.com

Received: February 14, 2025; Revised: February 24, 2025; Accepted: February 25, 2025; Published online: April 14, 2025

Abstract: This study explored the impact of heat stimulation on skin barrier damage, aging, and inflammatory responses by analyzing gene and protein-level changes. Additionally, it examined the restorative effects and regulatory mechanisms of red ginseng (RG) extract. The results demonstrated that heat stimulation decreased mRNA expression of the skin barrier markers, aquaporin 3 (AQP3), ceramide synthase 3 (CerS3), and occludin (OCL), while increasing the expression of matrix metalloproteinases (MMP)-1, MMP-2, and MMP-3, and proinflammatory factors such as interleukins IL-6 and IL-8, which are associated with skin damage. RG treatment modulated the expression of disrupted skin barrier markers (AQP3, CerS3, OCL), aging markers (MMP-1, -2, -3), and inflammatory factors (IL-6, IL-8), confirming the recovery-promoting effects against heat-induced skin damage. Mechanistic analysis revealed that both nuclear factor-kappa B (NF- κ B) and mitogen-activated protein kinase (MAPK) pathways were activated by heat stimulation, with NF- κ B activation suppressed by RG treatment. In conclusion, RG demonstrated the ability to restore skin integrity and alleviate damage.

Keywords: fibroblasts, heat stimulation, keratinocytes, red ginseng, skin damage

INTRODUCTION

Skin aging can be broadly divided into natural intrinsic aging associated with advancing years and extrinsic aging caused by UV rays [1]. A newly emergent concept in the field is thermal aging. Heat is a form of energy that can be transferred by direct contact conduction, circulating current convection, and infrared (IR) radiation from a heated object. Studies have extensively studied the characteristics and molecular mechanisms of heat-induced skin aging [2-4], showing that heat stimulation induces the expression of matrix metalloproteinases (MMPs). Heat stimulation activates extracellular signal-regulated kinase (ERK) and c-Jun N-terminal kinase (JNK) in human dermal fibroblasts (HDFs), increasing the expression of MMP-1 and MMP-3 [5]. Heat shock also affects the production of cytokines, including interleukins IL-6 and IL-12, and transforming growth factor (TGF)- β , which influence the regulation of extracellular matrix proteins. Heat stimulation increases MMP-12 in the

human dermis, and MMP13 in a hairless-mouse model [2,5-7]. It also increases reactive oxygen species (ROS) production and reduces the levels of the antioxidants that regulate oxidation reactions, such as glutathione (GSH), dehydrogenase 1 (NQO1), heme oxygenase (HO-1), and nuclear factor erythroid-derived 2-related factor 2 (NRF2) [8]. Although recent research has focused on skin aging caused by heat stimulation, the aging and inflammatory effects of such thermal exposure are also expected to affect the skin barrier.

Korean red ginseng (*Panax ginseng* Meyer), a popular traditional medicine in Asia, is well known for its anti-aging effects on the skin. Red ginseng can protect the epidermal and dermal layers of the skin from strong UV-B radiation. Through maltol, one of the phenolic components of red ginseng extract (RG), it reduces fatigue and exhibits antioxidant properties [9-12]. Additionally, the ginsenosides Re, Rc, and Rb1 present in RG induce the expression of procollagen-type

genes and reduce the expression of MMP-1 and tumor necrosis factor (TNF) [14-16]. In the hairless SKH-1 mouse model, administration of RG was reported to produce anti-photoaging effects, including increased epidermal thickness, inhibition of wrinkle formation, and decreased immunohistochemical density of myeloperoxidase, which is associated with inflammation in photoaged skin [17,19].

Red ginseng extract has been shown to suppress the production of inflammatory cytokines and chemokines, including IL-6 and IL-8, through the MAPK and NF- κ B pathways [18]. It also regulates procollagen type 1 and MMP-1 in hairless mouse models and enhances UVB resistance by promoting the production of propylparaben and filaggrin [13]. Previous studies suggest that RG extract may help prevent skin inflammation and restore the skin's protective barrier function.

Our study aimed to determine the ability of RG to promote recovery from heat-induced skin damage. This research attempts to elucidate the various types of skin damage caused by heat stimulation, including thermal aging, to shed light on the recovery-promoting effects of RG treatment in *in vitro* systems, and identify underlying molecular mechanisms.

MATERIALS AND METHODS

Preparation of RG

A free sample of RG powder was obtained from the Korea Ginseng Corporation (KGC) [<https://www.kgc.co.kr/en/index.do>] dissolved in DMSO.

Cell culture and heat stimulation

Normal human dermal fibroblasts (NHDFs), purchased from Lonza Ltd. (Basel, Switzerland), were grown in Fibroblast Basal Medium (FBM; Lonza Ltd.), supplemented with Bullet Kit (FGM-2 SingleQuot Kit Supplement & Growth Factors kit; Lonza Ltd.). The human low-calcium high temperature (HaCaT) keratinocyte cell line, kindly provided by Eulji University, was cultured in Dulbecco's Modified Eagle Medium (DMEM; Welgene, Gyeongsan, Gyeongsangbuk-do, Korea), containing 5% fetal bovine serum (FBS; Welgene), and 1% penicillin-streptomycin. Cells were

maintained at 37°C in a humidified 5% CO₂ atmosphere. For heat stimulation, HaCaT cells were seeded in a cell culture plate and kept in a water bath at 45°C for 10 min and then incubated for 24 h.

Cell viability

Cell viability (Supplementary Fig. S1) was determined using the WST-1 assay (EZ-Cytox; DoGenBio, Seoul, Korea) according to the manufacturer's instructions [20]. Briefly, cells were seeded in 96-well plates and cultured for 24 h. Test samples were added at different concentrations, and cells were incubated for 24 h. Thereafter, 100 μ L of medium containing 10 μ L of WST (water-soluble tetrazolium salt) solution was added to each well, and the plates were incubated for 1 h at 37°C. The absorbance of each well at 450 nm was measured using an absorbance microplate reader (Multiskan GO; Thermo Scientific, Waltham, MA, USA). Cell viability was determined according to the equation:

$$\text{Cell viability (\%)} = (\text{sample treatment group absorbance} / \text{control group absorbance}) \times 100.$$

Quantitative reverse transcription-polymerase chain reaction (RT-qPCR)

Total RNA was extracted using TRIzol solution (Invitrogen, Carlsbad, CA, USA) according to the manufacturer's instructions. First-strand cDNA was synthesized from 1 μ g of total RNA using the Transcriptor First Strand cDNA Synthesis Kit (Roche, Basel, Switzerland). Expression of select target genes in cDNA samples was quantified on a high-performance real-time PCR instrument (LightCycler 96 System; Roche), and their mRNA expression levels were normalized to that of glyceraldehyde 3-phosphate dehydrogenase (*GAPDH*; qHsaCID0015464). Target genes included those for aquaporin (qHsaCED0046291), ceramide synthase (qHsaCID0015946), MMP-1 (qHsaCED0048106), MMP-2 (qHsaCID0015623), and MMP-3 (qHsaCID0006170). Primers for target genes and *GAPDH* were purchased from Bio-Rad (Hercules, CA, USA). The cycling conditions were as follows: denaturation at 95°C for 10 min, followed by 45 cycles at 95°C for 10 s, 60°C for 10 s, and 75°C for 10 s. Gene expression was quantified using the comparative CT method [19]. All data were obtained from more than two independent experiments carried out in triplicate.

Quantitation of the proinflammatory cytokines, IL-6 and IL-8

HaCaT cells were seeded in 96-well plates at 1.5×10^4 cells/well, heat-stimulated for 10 min at 45°C after 24 h, and incubated for 24 h in a 37°C, 5% CO₂ incubator. Conditioned media (CM) for proinflammatory cytokine assays were harvested 24 h after RG treatment, and the concentrations of IL-6 and IL-8 in the culture media were determined using sandwich enzyme-linked immunosorbent assay (ELISA) kits (R&D Systems, Minneapolis, MN, USA) according to the manufacturer's instructions. ELISAs were analyzed using an absorbance microplate reader (Multiskan GO; Thermo Fisher Scientific, Waltham, MA, USA).

Quantitation of MMP-1 and procollagen

To stimulate MMP-1 production of NHDF, conditioned media (CM) was obtained by irradiating HaCaT cells with heat (45°C for 10 min) and culturing for 24h. NHDFs were seeded (0.6×10^4) in a 96-well plate, cultured for 24 h, replaced with supplement-free FBM, and cultured for another day. RG was diluted in CM into various concentrations, treated in NHDF, and cultured for 24 h; the supernatant was used for MMP-1 ELISA (R&D systems, Minneapolis, MN, USA). In the subsequent method, MMP-1 ELISA was performed according to the manufacturer's recommendations, and MMP-1 levels were quantified by measuring the absorbance at 450 nm. To perform procollagen ELISA, NHDFs were seeded at 0.6×10^4 in a 96-well plate, cultured for 24 h, replaced with supplement-free FBM, and cultured for another day. The positive control (TGF- β) and RG diluted in supplement-free FBM were treated with NHDF and incubated for 24 h, and the supernatant was used for ELISA (Procollagen ELISA; Takara Bio, Kusatsu, Shiga, Japan). In the subsequent method, Procollagen ELISA was performed according to the manufacturer's recommendations, and procollagen levels were quantified by measuring the absorbance at 450 nm.

Western blot analysis

Cells in culture dishes, heat-treated as described above, were directly lysed with RIPA buffer (Thermo Fisher Scientific, Waltham, MA, USA) supplemented with a cocktail of proteinase and phosphatase inhibitors

(Thermo Fisher Scientific). Cell lysates (30 mg) were resolved by sodium dodecyl sulfate-polyacrylamide gel electrophoresis (SDS-PAGE) on 4-12% gels and transferred to nitrocellulose membranes (Invitrogen, Carlsbad, CA, USA). The blots were washed with 10 mM Tris-HCl [pH 7.6], 150 mM NaCl, and 0.1% Tween-20 (TBST), blocked with 5% skim milk in TBST for 1 h at room temperature, and incubated for 12 h at 4°C with primary antibodies (diluted 1:1000) against phosphorylated p38 (p-p38), total p38, p-ERK, total ERK, p-JNK, total JNK and p-NF- κ B (Cell Signaling Technology, Danvers, MA, USA). The membranes were washed with TBST and incubated with horseradish peroxidase-conjugated goat anti-rabbit or goat anti-mouse IgG antibodies (Cell Signaling Technology, Danvers, MA, USA), diluted 1:10,000, for 1 h at room temperature. The bands were visualized using an enhanced chemiluminescence detection system (Amersham Biosciences, GE Healthcare, Buckinghamshire, UK) following the manufacturer's instructions.

Immunocytochemistry

HaCaT cells were seeded onto coverslips in 6-well plates (5×10^5 cells/well) and incubated for 24 h. After washing with 1 \times phosphate-buffered saline (PBS), the cells were serum-starved overnight and treated with 100 or 200 μ g/mL RG for 24 h. For immunocytochemistry, the cells were fixed for 10 min in 4% paraformaldehyde at 4°C, permeabilized with 0.1% Triton X-100 for 20 min, and blocked with 10% bovine serum albumin (BSA) for 30 min at room temperature. Cells were incubated overnight at 4°C with primary antibodies against occludin and p-NF- κ B (Cell Signaling Technology, Danvers, MA, USA), diluted in 3% BSA, followed by incubation at room temperature with Alexa Fluor 488-conjugated anti-rabbit IgG secondary antibody (Cell Signaling Technology, Danvers, MA, USA) in 3% BSA. Nuclei were counterstained with 4',6-diamidino-2-phenylindole (DAPI; Sigma Aldrich, St. Louis, MO, USA), and the slides were visualized using an inverted digital microscope (Eclipse Ts2-FL; Nikon, Japan)

Statistical analysis

The results are expressed as the means \pm standard deviation (SD). The data were analyzed using a Student's t-test, and a two-tailed P<0.05 was considered statistically significant.

RESULTS

Recovery-promoting effects of RG on skin damage caused by heat stimulation

Before examining the effects of RG on the response of skin cells to heat stimulation, we tested RG on HaCaT cells alone to determine the test concentration at which RG was not cytotoxic. Preliminary experiments identified 20 $\mu\text{g/mL}$ as a non-toxic RG concentration. Treatment of HaCaT cells with RG (20 $\mu\text{g/mL}$) resulted in a significant increase in mRNA expression levels

of aquaporin 3 (AQP3), ceramide synthase 3 (CerS3), and occludin (OCL) (Fig. 1A-C). To see if RG can alter tight junctions, we monitored the protein expression of the representative tight junction protein OCL. In addition to significantly upregulating OCL transcripts, as shown by real-time qPCR (Fig. 1C), RG increased the level of OCL proteins at the cell membrane, as shown by immunocytochemistry (Fig. 1D). These data suggest that RG enhances skin barrier function in heat-damaged skin by upregulating AQP3, CerS3, and OCL in epidermal keratinocytes.

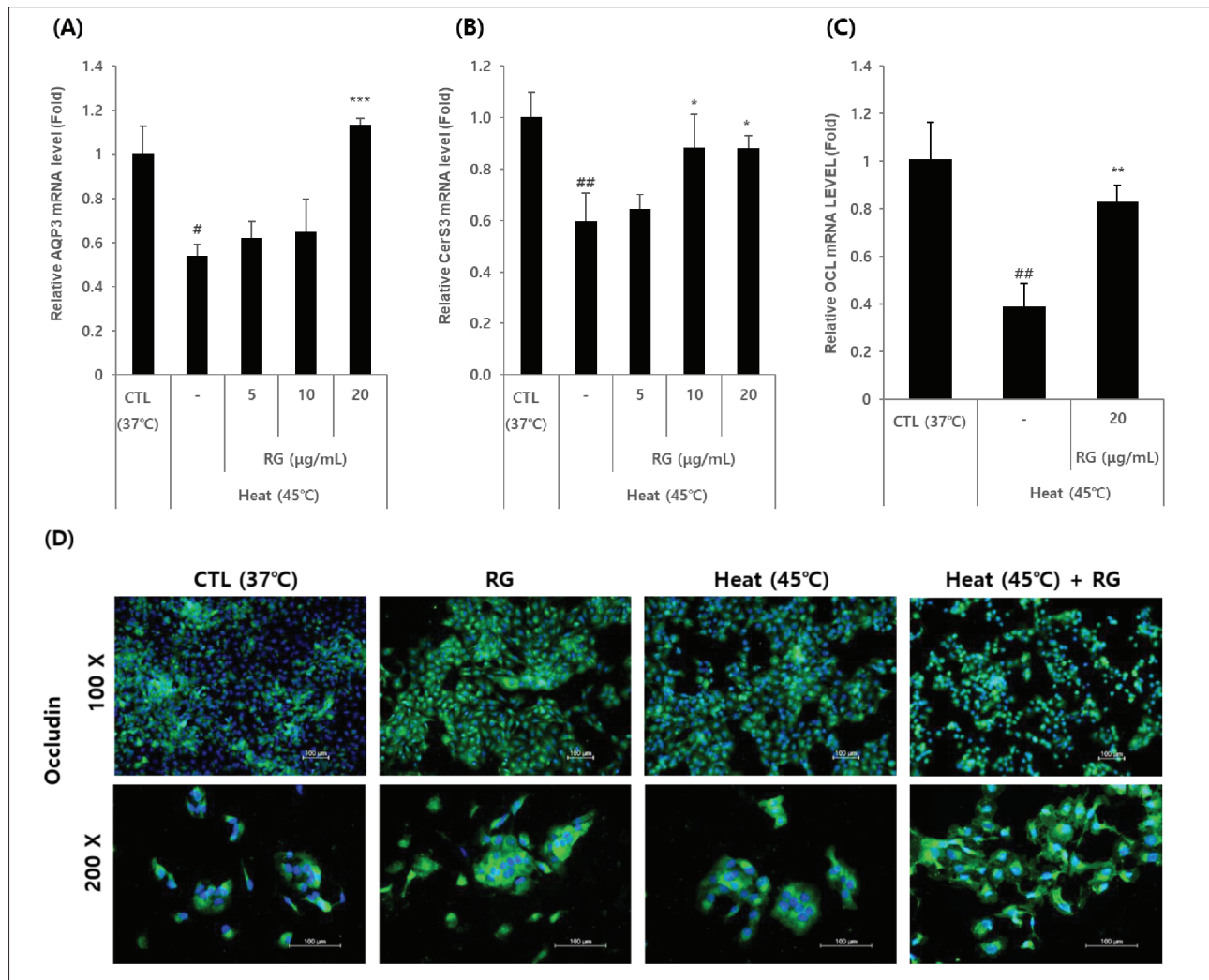


Fig. 1. The recovery-promoting effect of RG on skin damage caused by heat stimulation. **A, B, C** – Effects of RG on mRNA levels of AQP3, CerS3, and OCL in HaCaT cells. Cells were treated with 5 to 20 $\mu\text{g/mL}$ RG for 24 h. mRNA levels were determined by real-time qPCR and normalized to those of GAPDH. **D** – Effect of RG on OCL protein levels. Representative immunofluorescence staining of OCL in HaCaT cells. Green, OCL; blue, DAPI. Data are expressed as means \pm SD of at least three independent measurements. * P <0.05, ** P <0.01 vs control (CTL).

Effect of RG on protein levels of the inflammatory cytokines, IL-6 and IL-8, in HaCaT cells

To assess whether RG protects keratinocytes exposed to heat stimulation by exerting an anti-inflammatory effect, we briefly stimulated HaCaT cells with heat (45°C, 10 min), and 24 h later performed ELISA to analyze the culture media for secreted proinflammatory cytokines, IL-6 and IL-8. RG at a concentration of 520 µg/mL significantly inhibited the secretion of IL-6 and IL-8 in the culture supernatants of heat-stimulated HaCaT cells (Fig. 2A and B). These data indicate that RG has a potent anti-inflammatory effect on heat-stimulated keratinocytes.

Effect of RG on heat stimulation-induced changes in aging-related mRNA and protein levels in NHDFs

To evaluate the anti-aging effects of RG on dermal skin cells, we used primary NHDFs (Supplementary Fig. S1). First, we examined the mRNA expression levels of MMPs (MMP1, -2, and -3) in NHDFs treated with RG. As shown in Fig. 3A-C, heat stimulation increased

the expression of all MMP genes, producing an effect significantly attenuated by RG treatment. Next, we assessed the production of MMP-1 and procollagen in NHDFs treated with RG. To this end, we collected conditioned medium from NHDFs exposed to heat stimulation with or without RG treatment and evaluated the levels of secreted MMP-1, which degrades collagen fibers, using ELISA. This analysis revealed that heat treatment increased the levels of secreted MMP-1 in conditioned medium from NHDFs. However, this increase was significantly reduced by treatment with 20 µg/mL RG (Fig. 3D). RG caused a concentration-dependent increase in procollagen production in NHDFs (Fig. 3E). These results suggest that RG exerts a protective anti-aging effect on the dermis by inducing collagen synthesis and reducing MMP-1 production.

RG protects against heat-stimulated skin damage through the NF-κB signaling pathway but not the MAPK signaling pathway.

To identify the specific pathways underlying heat-induced skin damage and recovery by RG, we confirmed the expression of proteins involved in MAPK and

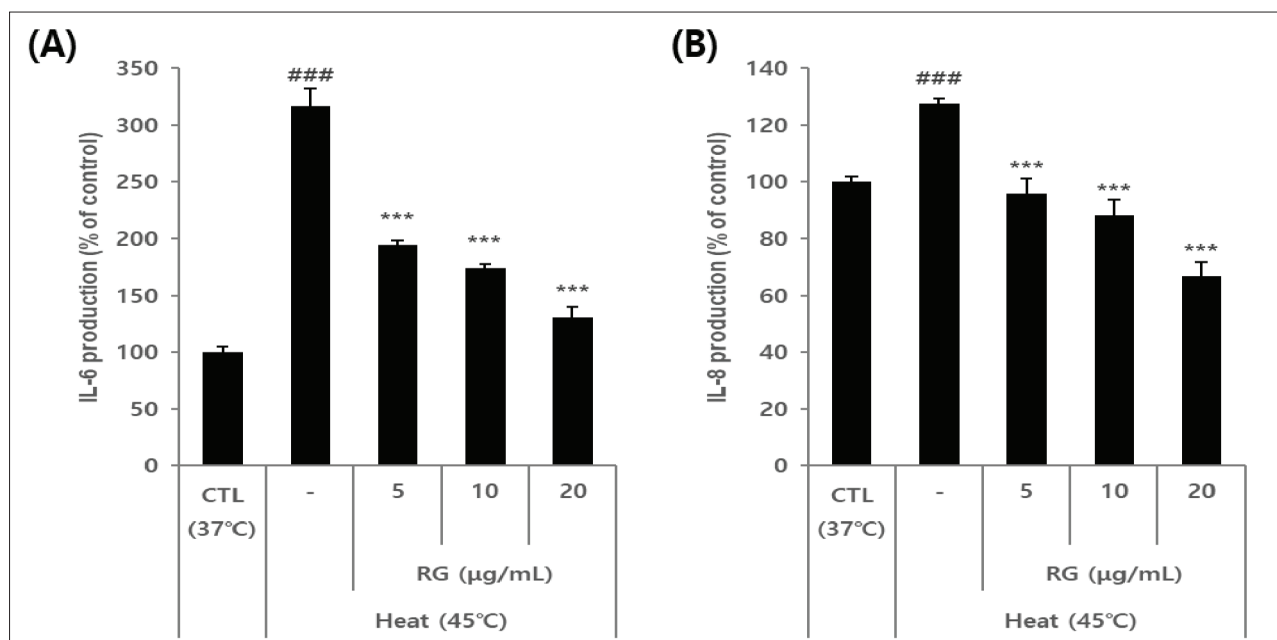


Fig. 2. Effects of RG on the inflammatory cytokines, IL-6 and IL-8, in HaCaT cells. **A, B** – Effects of RG on heat-stimulated production of IL-6 and IL-8 in HaCaT cells. Cells were treated with 5, 10, or 20 µg/mL RG for 24 h and then heat stimulated by exposure to 45°C for 10 min. The relative protein levels were estimated by ELISA. Data are presented as means±SD of at least three independent measurements. ####P<0.001 vs control (CTL); ***P<0.001 vs the heat stimulated-only group.

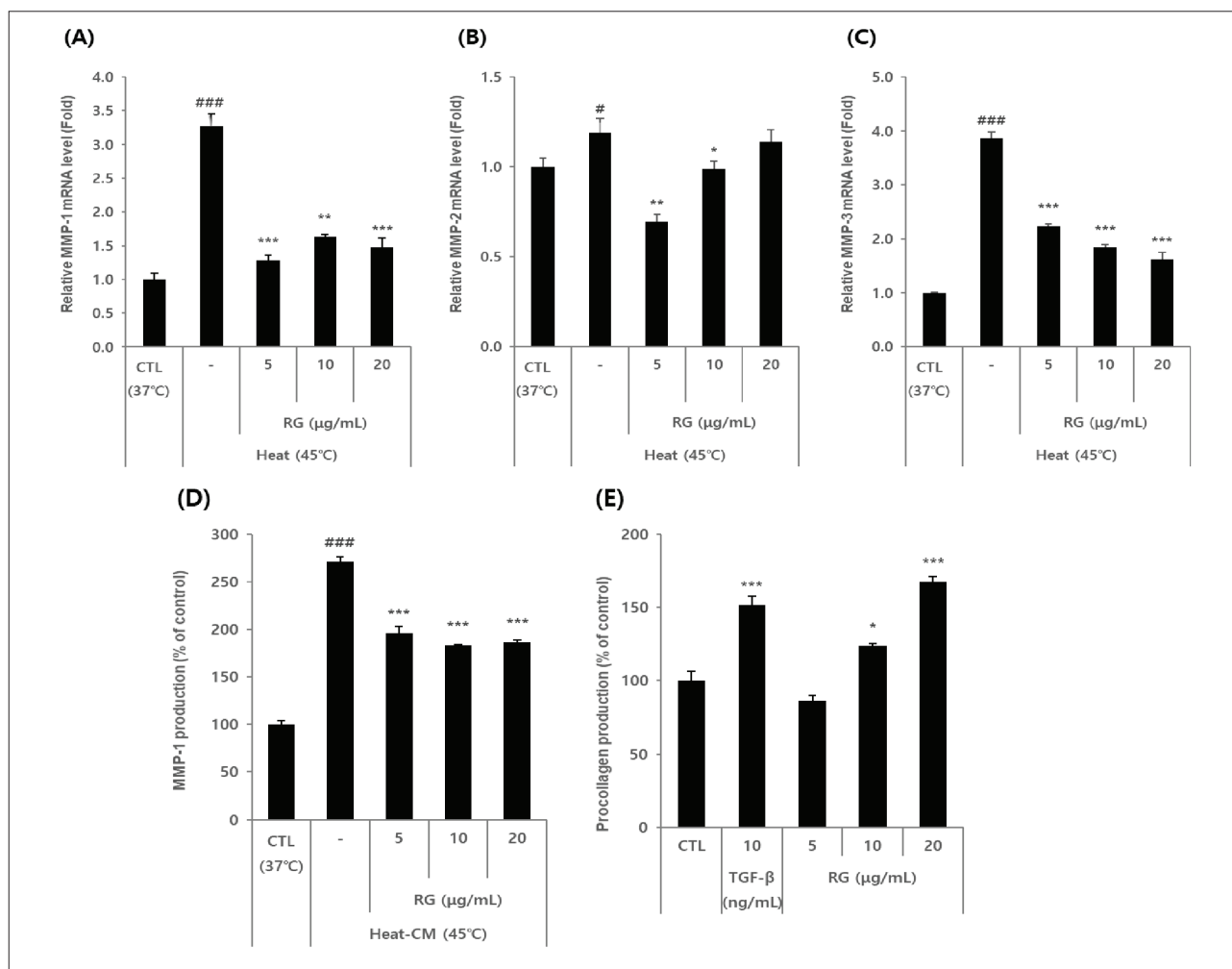


Fig. 3. Effects of RG on mRNA and protein levels of anti-aging markers. **A, B, C** – Effects of RG on the heat-stimulated production of MMP-1, MMP-2, and MMP-3 mRNA levels in NHDFs. Cells were treated with 5 to 20 µg/mL RG for 24 h. mRNA levels were determined by real-time qPCR and normalized to those of GAPDH. Data are expressed as means±SD of at least three independent measurements. ^{###}P<0.001 versus control (CTL); *P<0.05, **P<0.01, ^{***}P<0.001 vs the heat stimulated-only group. **D** – Effect of RG on MMP-1 production in NHDFs. NHDFs were treated with 5, 10, or 20 µg/mL RG in conditioned media (CM) from heat-stimulated (45°C, 10 min) irradiated. MMP-1 production was determined by ELISA. **E** – Effect of RG on procollagen production in NHDFs. Cells were treated with 5, 10, and 20 µg/mL RG and TGF-β for 24 h as described in D; procollagen levels were determined by ELISA. Data are presented as means±SD. ^{###}P<0.001 compared with the control (CTL); ^{***}P<0.001 vs CM (D). ^{***}P<0.001 vs TGF-β (E).

NF-κB signaling pathways. As shown in Fig. 4A, heat stimulation increased phosphorylated p38, JNK, and ERK. Treatment with RG did not decrease the levels of phosphorylated MAPK pathway proteins following heat treatment. We also confirmed that heat stimulation increased the levels of phosphorylated NF-κB. In this case, however, the increase was attenuated by treatment with RG (Fig. 4B). These results were also confirmed by immunofluorescence analysis of p-NF-κB p65 levels 30 min after heat stimulation (Fig. 4C).

DISCUSSION

Previous studies focusing mainly on photo-aging and the inflammation-promoting effects of UV rays have demonstrated the pharmacological effects of RG on skin [14-17,19,22]. However, few studies have investigated skin and skin barrier damage caused by heat, including IR and UV radiation, making it an emerging concept in the field [23]. Therefore, we sought to identify new mechanisms through which RG controls skin damage by applying different experimental techniques to

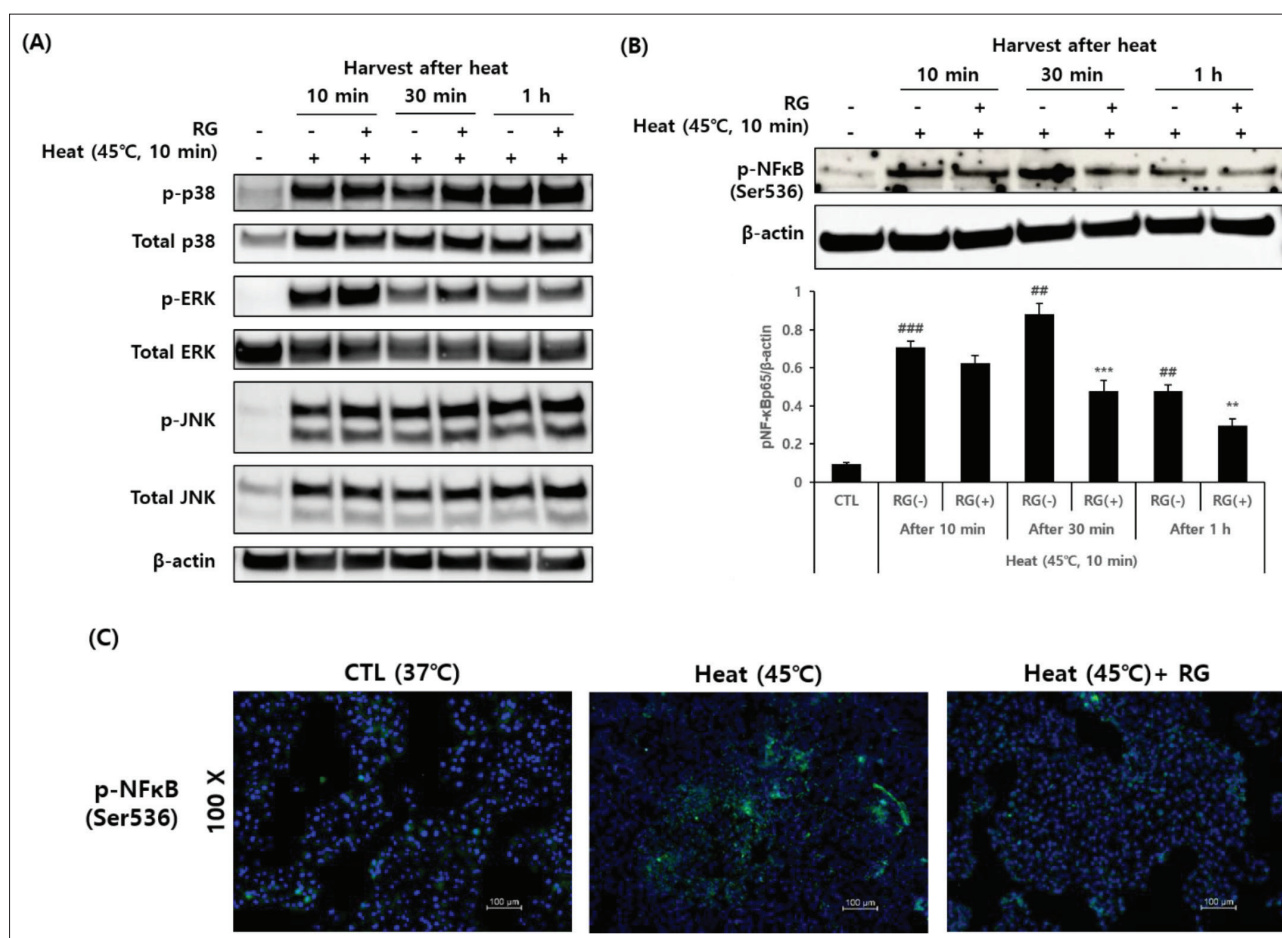


Fig. 4. Expression of proteins involved in MAPK and NF-κB signaling pathways during RG treatment in response to heat stimulation. **A** – Western blot analysis of MAPK pathway protein expression in heat-stimulated keratinocytes treated with or without RG. **B** – Western blot analysis and quantification of p-NF-κB P65 expression in heat-stimulated keratinocytes treated with or without RG. **C** – Immunofluorescence detection of p-NF-κB P65 30 min after heat stimulation. ## $P < 0.01$, ### $P < 0.001$ compared with the control (CTL); ** $P < 0.01$, *** $P < 0.001$ vs RG (-).

monitor the suppression and improvement in skin barrier damage, inflammation, and aging caused by heat stimulation.

The heat stimulation experimental model used in this study confirmed the previously established link between skin barrier damage, aging, and inflammation. Specifically, we found that heat stimulation reduced the expression of the gene encoding OCL [24], which has a role in tightening the binding between factor cells and cells related to the skin barrier – CerS3 [25], with a role in producing ceramide, a lipid important for the transmission of cell signals, and AQP3 [26], which is involved in moisturizing the skin and maintaining intracellular water balance. In addition, heat stimulation increased the expression of the inflammatory

cytokines, IL-6 and IL-8, causing an inflammatory response. It also increased expression of the matrix metalloproteinases, MMP-1, MMP-2, and MMP-3, which are involved in aging. Treatment with RG restored the heat-induced suppression of OCL, CerS3, and AQP3 gene expression, confirming its ability to alleviate skin barrier damage and moisture loss caused by heat stimulation. RG suppressed the heat-induced upregulation of MMP-1, MMP-2, and MMP-3 gene expression, inhibited MMP-1 protein production, and enhanced procollagen production, thereby inhibiting aging. In addition, RG was also shown to suppress the increase in IL-6 and IL-8 production induced by heat stimulation, thereby suppressing the associated inflammatory response.

To confirm the underlying mechanism, we used Western blotting to analyze the expression of proteins involved in NF- κ B and MAPK pathways, which are the main signaling pathways that mediate inflammation. We confirmed that heat stimulation increased the expression of the MAPK pathway proteins JNK, ERK, and p38 but RG did not reduce their upregulation. The activation of NF- κ B, which was also increased by heat stimulation (as evidenced by an increase in its phosphorylated form), was attenuated by treatment with RG, a finding confirmed by immunocytochemical analyses. These observations suggest that the anti-inflammatory, anti-aging, and skin barrier recovery-promoting effects of RG treatment following heat stimulation are attributable to inhibition of the NF- κ B pathway, but not the MAPK pathway.

Unlike ginseng and white ginseng, RG undergoes a steaming process that increases the content of some ginsenosides such as Rg2, Rg3, and Rh1 [27]. The content of ginsenosides in RG can vary depending on the specific steaming process used. These ginsenosides, which play an important role in controlling the inflammatory response, have been shown to affect both the MAPK and NF- κ B pathways [28-29]. Previous studies have reported that ginsenosides Rg2, Rg3, and Rh1 inhibit the MAPK pathway [29]; our findings do not align with these results. However, since we did not conduct a ginsenoside content analysis of our RG sample, and because different ginsenosides may have varying effects on specific pathways, we cannot definitively conclude how the ratios of ginsenosides contribute to the observed inhibition of the NF- κ B pathway, but not the MAPK pathway, in the recovery-promoting effects of our RG preparation.

In conclusion, our results confirmed that RG exerts recovery-promoting and skin damage-alleviating effects and suppresses inflammatory reactions and aging by inhibiting NF- κ B activation. Because the composition or ratio of ginsenosides can influence the potential synergy of RG components, these findings should be validated through an analysis of the RG composition.

Funding: This work was supported by the 2022 Grant from The Korean Society of Ginseng.

Author contributions: JY Kim and WJ Bang contributed equally to this work. Conceptualization: CS Lee. Methodology: JY Kim, WJ Bang; data curation: JY Kim and WJ Bang; writing, original

draft preparation: JY Kim, WJ Bang, and CS Lee; writing, review, and editing: CS Lee; supervision: CS Lee. All authors have read and agreed to the published version of the manuscript.

Conflict of interest disclosure: The authors report no conflicts of interest related to this work.

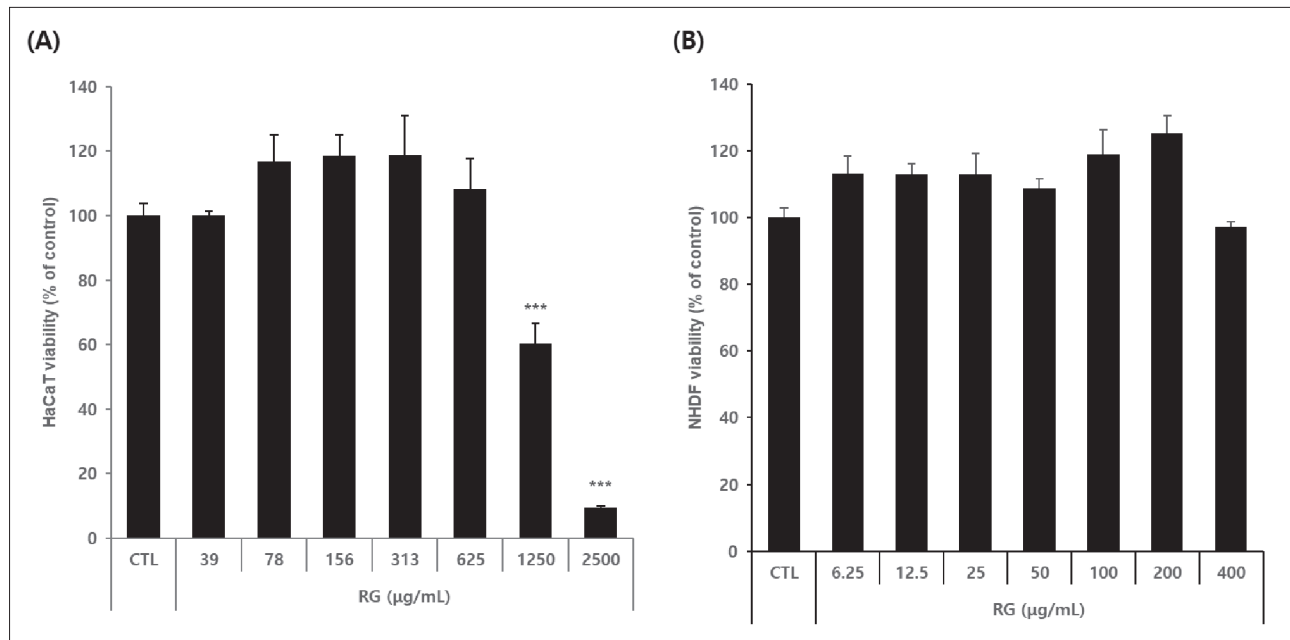
Data availability: The raw data underlying this article is available as an online supplementary research dataset: https://www.serbiosoc.org.rs/NewUploads/Uploads/Kim%20et%20al_Research%20Dataset.pdf

REFERENCES

- Farage MA, Miller KW, Elsner P, Maibach HI. Intrinsic and extrinsic factors in skin ageing: a review. *Int J Cosmet Sci.* 2008;30(2):87-95. <https://doi.org/10.1111/j.1468-2494.2007.00415.x>
- Seo JY, Chung JH. Thermal aging: a new concept of skin aging. *J Dermatol Sci.* 2006;2(1):S13-22. <https://doi.org/10.1016/j.descs.2006.08.00>
- Kim JE, Shin MH, Chung JH. Epigallocatechin-3-gallate prevents heat shock-induced MMP-1 expression by inhibiting AP-1 activity in human dermal fibroblasts. *Arch Dermatol Res.* 2013;305:595-602. <https://doi.org/10.1007/s00403-013-1393-y>
- Lee YM, Li WH, Kim YK, Kim KH, Chung JH. Heat-induced MMP-1 expression is mediated by TRPV1 through PKC α signaling in HaCaT cells. *Exp Dermatol.* 2008;17(10):864-870. <https://doi.org/10.1111/j.1600-0625.2008.00738.x>
- Park CH, Lee MJ, Ahn J, Kim S, Kim HH, Kim KH, Chung JH. Heat shock-induced matrix metalloproteinase (MMP)-1 and MMP-3 are mediated through ERK and JNK activation and via an autocrine interleukin-6 loop. *J Invest Dermatol.* 2004;123(6):1012-9. <https://doi.org/10.1111/j.0022-202X.2004.23487.x>
- Chen Z, Seo JY, Kim YK, Lee SR, Kim KH, Cho KH, Chung JH. Heat modulation of tropoelastin, fibrillin-1, and matrix metalloproteinase-12 in human skin in vivo. *J Invest Dermatol.* 2005;124(1):70-8. <https://doi.org/10.1111/j.0022-202X.2004.23550.x>
- Cho S, Shin MH, Kim YK, Seo JE, Lee YM, Park CH, Chung JH. Effects of infrared radiation and heat on human skin aging in vivo. *J Investig Dermatol Symp Proc.* 2009;14(1):15-9. <https://doi.org/10.1038/jidsymp.2009.7>
- Son D, Kim M, Woo H, Park D, Jung E. Anti-Thermal Skin Aging Activity of Aqueous Extracts Derived from Apple Mint (*Mentha suaveolens* Ehrh.) in Human Dermal Fibroblasts. *J Evid Based Complementary Altern Med.* 2018;(1):4595982. <https://doi.org/10.1155/2018/4595982>
- Park MY, Han SJ, Moon D, Kwon S, Lee JW, Kim KS. Effects of red ginseng on the elastic properties of human skin. *J Ginseng Res.* 2020;44(5):738-46. <https://doi.org/10.1016/j.jgr.2019.08.004>
- Park SY, Shin YK, Kim HT, Kim YM, Lee DG, Hwang E, Yi TH. A single-center, randomized, double-blind, placebo-controlled study on the efficacy and safety of "enzyme-treated red ginseng powder complex (BG11001)" for antiwrinkle and

- proelasticity in individuals with healthy skin. *J Ginseng Res.* 2016;40(3):260-8. <https://doi.org/10.1016/j.jgr.2015.08.006>
11. Jeon JM, Choi SK, Kim YJ, Jang SJ, Cheon JW, Lee HS. Antioxidant and antiaging effect of ginseng berry extract fermented by lactic acid bacteria. *J Soc Cosmet Sci Korea.* 2011;37(1):75-81. <https://doi.org/10.15230/SCSK.2011.37.1.075>
 12. Lee CH, Kim HI, Kim JS, Oh MJ, Kim SW, Ma SY, Oh CH. Morphological studies on the inhibitory effects of photoaging skin of fermented red ginseng in hairless mice. *J Physiol Pathol Korean Med.* 2014;28(2):206-6. <https://doi.org/10.15188/kjopp.2014.04.28.2.206>
 13. Hong CE, Lyu SY. Anti-inflammatory and anti-oxidative effects of Korean red ginseng extract in human keratinocytes. *Immune Netw.* 2011;11(1):42. <https://doi.org/10.4110/in.2011.11.1.42>
 14. Hwang E, Lee TH, Park SY, Yi TH, Kim SY. Enzyme-modified Panax ginseng inhibits UVB-induced skin aging through the regulation of procollagen type I and MMP-1 expression. *Food Funct.* 2014;5(2):265-74. <https://doi.org/10.1039/C3FO60418G>
 15. Lee J, Jung E, Lee J, Huh S, Kim J, Park M, Park D. Panax ginseng induces human Type I collagen synthesis through activation of Smad signaling. *J Ethnopharmacol.* 2007;109(1):29-34. <https://doi.org/10.1016/j.jep.2006.06.008>
 16. So SH, Lee SK, Hwang EI, Koo BS, Han GH, Kim NM. Effects of Korean red ginseng and herb extracts mixture (KTNG0345) on procollagen biosynthesis and matrix metalloproteinase-1 activity in human dermal fibroblast. *J Ginseng Res.* 2007;31(4):196-202. <https://doi.org/10.5142/JGR.2007.31.4.196>
 17. Truong VL, Bae YJ, Bang JH, Jeong WS. Combination of red ginseng and velvet antler extracts prevents skin damage by enhancing the antioxidant defense system and inhibiting MAPK/AP-1/NF- κ B and caspase signaling pathways in UVB-irradiated HaCaT keratinocytes and SKH-1 hairless mice. *J Ginseng Res.* 2024;48(3):323-32. <https://doi.org/10.1016/j.jgr.2024.01.003>
 18. Kee JY, Jeon YD, Kim DS, Han YH, Park J, Youn DH, Kim SJ, Ahn KS, Um JY, Hong SH. Korean Red Ginseng improves atopic dermatitis-like skin lesions by suppressing expression of proinflammatory cytokines and chemokines in vivo and in vitro. *J Ginseng Res.* 2017;41(2):134-43. <https://doi.org/10.1016/j.jgr.2016.02.003>
 19. Kim HI, Oh MJ, Kim JS, Lee SC, Kwon J, Lee CH. Protective effect of fermented red ginseng extracts on photoaging skin of induced by UVB in hairless mice. *J Physiol & Pathol Korean Med.* 2015;29(1):58-65. <https://doi.org/10.15188/kjopp.2015.02.29.1.58>
 20. Banerjee T, Aggarwal M, Sommers JA, Brosh Jr RM. Biochemical and cell biological assays to identify and characterize DNA helicase inhibitors. *Methods.* 2016;108:130-41. <https://doi.org/10.1016/j.ymeth.2016.04.007>
 21. Livak KJ, Schmittgen TD. Analysis of relative gene expression data using real-time quantitative PCR and the 2- $\Delta\Delta$ CT method. *Methods.* 2001;25(4):402-8. <https://doi.org/10.1006/meth.2001.1262>
 22. You L, Cho JY. The regulatory role of Korean ginseng in skin cells. *J Ginseng Res.* 2021;45(3):363-70. <https://doi.org/10.1016/j.jgr.2020.08.004>
 23. Choi W, Cho JH, Park SH, Kim DS, Lee HP, Kim D, Kim HS, Kim JH, Cho JY. Ginseng root-derived exosome-like nanoparticles protect skin from UV irradiation and oxidative stress by suppressing activator protein-1 signaling and limiting the generation of reactive oxygen species. *J Ginseng Res.* 2024;48(2):211-9. <https://doi.org/10.1016/j.jgr.2024.01.001>
 24. Odenwald MA, Turner JR. The intestinal epithelial barrier: a therapeutic target?. *Nat Rev Gastroenterol Hepatol.* 2017;14(1):9-21. <https://doi.org/10.1038/nrgastro.2016.169>
 25. Rabionet M, Gorgas K, Sandhoff R. Ceramide synthesis in the epidermis. *Biochim Biophys Acta Mol Cell Biol Lipids.* 2014;1841(3):422-34. <https://doi.org/10.1016/j.bbalip.2013.08.011>
 26. Hara-Chikuma M, Verkman AS. Aquaporin-3 facilitates epidermal cell migration and proliferation during wound healing. *J. Mol. Med.* 2008;86:221-31. <https://doi.org/10.1007/s00109-007-0272-4>
 27. Koh E, Jang OH, Hwang KH, An YN, Moon B. Effects of Steaming and Air-Drying on Ginsenoside Composition of Korean Ginseng (*Panax ginseng* CA Meyer). *J Food Process Preserv.* 2015;39(2):207-13. <https://doi.org/10.1111/jfpp.12412>
 28. Gao H, Kang N, Hu C, Zhang Z, Xu Q, Liu Y, Yang S. Ginsenoside Rb1 exerts anti-inflammatory effects in vitro and in vivo by modulating toll-like receptor 4 dimerization and NF- κ B/MAPKs signaling pathways. *Phytomedicine.* 2020;69:153197. <https://doi.org/10.1016/j.phymed.2020.153197>
 29. Xue Q, He N, Wang Z, Fu X, Aung L. HH, Liu Y, Yu T. Functional roles and mechanisms of ginsenosides from *Panax ginseng* in atherosclerosis. *J Ginseng Res.* 2021;45(1):22-31. <https://doi.org/10.1016/j.jgr.2020.07.002>

SUPPLEMENTARY MATERIAL



Supplementary Fig. S1. Effects of RG on keratinocyte (HaCaT) and Normal Human Dermal Fibroblast (NHDF) cell viability after 24 h treatment. **A, B** – Effects of RG on HaCaT and NHDF cell viability, respectively, after 24 h treatment. Cell viability rates were evaluated using the WST-1 assay. Data are presented as means±SD. ***P<0.001 vs control (CTL).

ONLINE SUPPLEMENTARY MATERIAL

The raw data underlying this article is available as an online supplementary research dataset:

https://www.serbiosoc.org.rs/NewUploads/Uploads/Kim%20et%20al_Research%20Dataset.pdf